Journal of Thermal Analysis, Vol. 41 (1994) 357-385

In celebration of the 60th birthday of Dr. Andrew K. Galwey

KINETICS OF THE THERMAL DEHYDRATIONS AND DECOMPOSITIONS OF SOME MIXED METAL OXALATES

A. Coetzee, M. E. Brown, D. J. Eve and C. A. Strydom*[1]

Chemistry Department, Rhodes University, Grahamstown 6140, South Africa
[1]Chemistry Department, University of Pretoria, Pretoria 0002, South Africa

Abstract

Both isothermal and programmed temperature experiments have been used to obtain kinetic parameters for the dehydrations and the decompositions in nitrogen of the mixed metal oxalates: $FeCu(ox)_2 \cdot 3H_2O$, $CoCu(ox)_2 \cdot 3H_2O$ and $NiCu(ox)_2 \cdot 3.5H_2O$, [$ox = C_2O_4$]. Results are compared with those reported for the thermal decompositions of the individual metal oxalates, Cuox, $Coox \cdot 2H_2O$, $Niox \cdot 2H_2O$ and $Feox \cdot 2H_2O$. X-ray photoelectron spectroscopy (XPS) was also used to examine the individual and the mixed oxalates.

Dehydrations of the mixed oxalates were mainly deceleratory processes with activation energies (80 to 90 $kJ \cdot mol^{-1}$), similar to those reported for the individual hydrated oxalates. Temperature ranges for dehydration were broadly similar for all the hydrates studied here (130 to 180°C).

Decompositions of the mixed oxalates were all complex endothermic processes with no obvious resemblance to the exothermic reaction of Cuox, or the reactions of physical mixtures of the corresponding individual oxalates.

The order of decreasing stability, as indicated by the temperature ranges giving comparable decomposition rates, was $NiCu(ox)_2 > CoCu(ox)_2 > FeCu(ox)_2$, which also corresponds to the order of increasing covalency of the Cu-O bonds as shown by XPS.

Keywords: decomposition, dehydration, DSC, EGA kinetics, mixed metal oxalates, TG, TM

Introduction

The thermal decompositions of metal oxalates have been studied extensively and various mechanisms of decomposition have been proposed [1].

* To whom correspondence should be addressed

John Wiley & Sons, Limited, Chichester
Akadémiai Kiadó, Budapest

The thermal behaviour of the mixed metal oxalates, $FeCu(ox)_2 \cdot 3H_2O$, $CoCu(ox)_2 \cdot 3H_2O$, and $NiCu(ox)_2 \cdot 3.5H_2O$, [$ox = C_2O_4$] has been examined using thermogravimetry (TG), thermomagnetometry (TM), differential scanning calorimetry (DSC) and evolved gas analysis (EGA) [2]. Results were compared with the thermal behaviour of the individual metal oxalates, Cuox, $Coox \cdot 2H_2O$, $Niox \cdot 2H_2O$ and $Feox \cdot 2H_2O$.

All three mixed oxalates, $MCu(ox)_2 \cdot xH_2O$, underwent dehydration prior to decomposition. Onset temperatures for dehydration in N_2 at 20 $deg \cdot min^{-1}$ were Co ($-3H_2O$): 140°C, Fe ($-3H_2O$): 140°C and Ni ($-3.5H_2O$): 200°C. The stoichiometries and thermochemistry of the dehydrations are summarised in Table 2 of Ref. [2]. The decompositions of the three mixed oxalates in N_2 all take place in two overlapping endothermic stages. The stoichiometries and thermochemistry [2] are summarised in Table 1.

Table 1 Stoichiometry and thermochemistry of the decompositions of the mixed oxalates in nitrogen [2]

Compound		Residue /%	Main solid products	ΔH (decomposition) / $kJ \cdot mol^{-1}$
Cuox	291	44.1	$Cu+Cu_2O$	-32.6±0.1
$FeCu(ox)_2$	299	40.0	$FeO+1/2Cu_2O$	160.0±6.0
$CoCu(ox)_2$	316	35.1	Cu+Co	97.1±9.7
$NiCu(ox)_2$	362	32.3	Cu+Ni	158.0±5.0

The mixed oxalates, $MCu(ox)_2 \cdot xH_2O$, do not show the exothermic thermal behaviour characteristic of Cuox [2–4].

A considerable amount of information on the kinetics of thermal dehydration and thermal decomposition of the related individual oxalates has been reported [4–17]. This information is summarized in Tables 2 and 3.

Experimental

Preparations

Samples were prepared and characterised as described in Ref. [2]. DSC curves for the Fe and Co mixed oxalates in N_2 showed the presence of a small proportion of co-precipitated Cuox as a physical mixture [2].

Table 2 Kinetic parameters for the dehydrations of the individual oxalates

T-range/°C	Model	α-range	E_a/kJ·mol^{-1}	ln(A/s^{-1})	Ref.
Feox·2H$_2$O					
165–185	R2(1)	0.23–0.90	87±12	16.5±0.1	[5]
	R2(2)	0.47–0.93	93±12	18.2±0.1	
	R3(1)	0.23–0.90	79±14	14.2±0.1	
	(3)	0.30–0.89	75±17	14.4±0.2	
prog T 1 deg·min^{-1}	R3	0.04–0.99	106±2	21.9	[6]
Coox·2H$_2$O					
prog T 1 deg·min^{-1}	F1	0.04–0.94	158±1	36.2	[6]
prog T 10 deg·min^{-1}	Coats & Redfern		91.7	20.4	[7]
	F1		92.0	21.3	
	R2		89.5	19.9	
	R3		90.0	19.6	
Niox·2H$_2$O					
180–205	R2	0.20–0.90	68±15	9.8±0.2	[5]

(1) From $f(\alpha)$ *vs.* t
(2) From v *vs.* t
(3) From ln v *vs.* ln(1–α)

Table 3 Kinetic characteristics of the decompositons of the individual oxalates

Oxalates	Isothermal T range/°C	Conditions	Models [19]	α range	E_a/kJ·mol^{-1}	ln(A/s^{-1})	Ref.
Cuox	247–272	accumulatory	A3	0.2–0.95	136		[4]
			R3	0.68–0.93			
			P1 (n=2.9)	<0.50			
			F1	>0.80			
	242–277	accumulatory	E1	0.01–0.30	140±7		[9]
			F1	0.24–0.91	180±7		
	235–261	vacuum	B1				[4]
			An (n=3.57)		128		
		N_2	A2		193	33.3	[8]
		air			184	31.9	
		N_2	independent	0.1–0.9	214	39.6	
Feox	330–350	N_2	R3	0.1–0.9	141±22	18.6	[5]
		accumulatory	A2	0.02–0.87	175±7		[10]
Coox	297–315	vacuum	induction period		204		[11]
dehydrated at 150°C			E1	0–0.50			
			linear	0.5–0.9			
			F1	0.90–0.95			
dehydrated at 200°C			induction period		225		
			E1	0–0.50			
				0.25–0.95	165		

Table 3 Continued

Oxalates	Isothermal T range/°C	Conditions	Models [19]	α range	E_a/kJ·mol^{-1}	ln(A/s^{-1})	Ref.
Coox							
coarse	317–427						
	(<352°C)		A2		159		[12]
	(>352°C)				57		
fine	(<392°C)		A3		120		
	(>392°C)				59		
Niox	245–260	accumulatory	R2 initial reaction	0–0.0085	141		[13]
(hydrate)			A2	0.10–0.85	210		
		differential	A2	0.20–0.88	130		
(dehydrated)				0.05–0.80	138		
	230–260	vacuum	R2 initial	<0.016	159		[14]
			Induction period		216		
			P1 (n=3 later n=2)		151		
	270–380	N_2	A2				[15]
			F1				
	253–360	vacuum	P1 (n=2)		121		[16]
			F1		136		
		vacuum	B1	0.01–0.5	141		[17]
			R3	0.5–0.98	148		

Thermal analysis

Dehydrations and decompositions of the oxalate samples were studied using thermogravimetry (TG) and differential scanning calorimetry (DSC), in both isothermal and programmed temperature modes, on Perkin Elmer Delta Series 7 instruments, in nitrogen or oxygen atmospheres. Platinum sample pans and sample masses of 1–5 mg were used for TG, and aluminium sample pans, covered but not crimped, for DSC.

The temperature range over which a series of isothermal DSC traces can be recorded is limited by the requirement that the rate of absorption or evolution of heat must be sufficient for the DSC signal to be clearly distinguishable from the baseline. The range required is thus often slightly higher and shorter than the optimum range for isothermal TG and direct comparisons of DSC and TG traces at the same temperature are often difficult.

In some of the experiments, the gas outlet of the DSC was connected to a thermal conductivity detector (TCD) with an optional cold trap, for monitoring the evolved gases [2].

Kinetic analysis

TG and DSC curves were converted to curves of fractional reaction (α) *vs.* time or temperature after importing the data files into a spreadsheet (LOTUS 1–2–3). α was calculated from either the fractional mass loss (TG), or the fractional area under the DSC curves. Derivatives were calculated using a nine-point Savitsky-Golay function [18].

Our data base for kinetic analysis thus consisted of: (i) sets of isothermal α – time curves; (ii) sets of isothermal rate ($d\alpha/dt$) – time curves; (iii) nonisothermal α – temperature curves; for (a) dehydration of the individual oxalates; (b) decomposition of the individual oxalates; (c) dehydration of the mixed oxalates; (d) decomposition of the mixed oxalates.

Isothermal studies:

The kinetic model which gave the best description of the isothermal results was determined by one or more of several methods [19]:

(1) From examination of the linearity of plots of $f(\alpha)$ *vs.* t, over as wide a range of α as possible. Rate coefficients at each isothermal temperature were then calculated from the slopes of these linear regions and used in Arrhenius plots to estimate activation energies and pre-exponential factors.

(2) From examination of the isothermal rate ($v = d\alpha/dt$) *vs.* time, t, curves. For the mixed oxalates (see more detail below), at least two overlapping rate processes were apparent. The shapes of the peaks indicated that both processes were initially acceleratory, passed through maxima (at different times) and then decelerated to completion (at different times). The Avrami-Erofeev equation, which is the most useful kinetic expression for describing such sigmoid α-time relationships, leads to rate-time expression of the form [20]:

$$v = nk^n t^{(n-1)} \exp(-(kt)^n) \quad (1)$$

For concurrent processes, the overall isothermal rate, v, was assumed to be made up of contributions v_1, v_2,...,v_i from the individual processes, combined with weighting factors, w_1, w_2,...,w_i, so that:

$$v = w_1v_1 + w_2v_2...+w_iv_i \quad (2)$$

where each of the contributions, v_i, has the form of Eq. (1), with individual values k_i and n_i for each process i.

Experimental v, t values (corrected if necessary for a time delay, t_o, so that $t' = t - t_o$) were then compared with calculated v, t values and the sums of the squares of the residuals,

$$S_v = \sum R_v = \sum (v_{exp} - V_{calc})^2 \text{ and } S_\alpha = \sum R_\alpha = \sum (\alpha_{exp} - \alpha_{calc})^2$$

were minimised by adjustment of n_i, k_i, w_i and, if necessary, t_o, to give a reasonable visual match of experimental and calculated v, t and α, t curves. Values of n control the shapes of the peaks and values of k and t_o determine the height and position of the peak on the time scale. Values of k and the isothermal temperatures were used in Arrhenius plots, as described above, to calculate E_a and A.

Application of the above analysis showed that generally the earlier processes could be fitted by sigmoid models, but the final process was decelerator. Information about the final decay process could be obtained by using method (1) above on the α – time curves obtained from the isothermal experiments.

Programmed temperature studies

Programmed temperature TG and DSC curves were converted to α – temperature curves, and kinetic parameters were estimated, using the Borchardt and Daniels [21] method. The linearity of plots of $\ln [d\alpha/dT)/(1-\alpha)^n]$ *vs.* $1/T$ for selected values of n, was examined and, if this was acceptable, the slopes were

Table 4 XPS peak binding energies (eV) of the individual and mixed oxalates (All values corrected for charging effects)

Peak	CuC_2O_4	FeC_2O_4	$FeCu(C_2O_4)_2$	NiC_2O_4	$NiCu(C_2O_4)_2$	CoC_2O_4	$CoCu(C_2O_4)_2$
Cu $2p_{3/2}$	932.35	–	932.35	–	932.85	–	932.05
Cu $2p_{1/2}$	952.15	–	952.65	–	952.35	–	951.90
Cu 2p multiplet splitting	19.80	–	20.30	–	19.50	–	19.85
Cu LMM	336.45	–	336.7	–	334.85	–	336.25
α' (Cu)	1849.50	–	1849.25	–	1851.60	–	1849.40
Fe $2p_{3/2}$	–	710.70	709.75	–	–	–	–
Fe $2p_{1/2}$	–	724.65	too small	–	–	–	–
Fe 2p multiplet splitting	– – –	13.95	–	–	–	–	–
Fe LVV	–	551.15	550.55	–	–	–	–
α' (Fe)	–	1413.15	1412.80	–	–	–	–

Table 4 Continued

Peak	CuC_2O_4	FeC_2O_4	$FeCu(C_2O_4)_2$	NiC_2O_4	$NiCu(C_2O_4)_2$	CoC_2O_4	$CoCu(C_2O_4)_2$
Co $2p_{3/2}$	–	–	–	–	–	782.60	781.25
Co $2p_{1/2}$	–	–	–	–	–	798.25	798.05
Co 2p multiplet splitting	–	–	–	–	–	15.65	16.80
Co LVV	–	–	–	–	–	483.85	483.85
α′ (Co)	–	–	–	–	–	1552.35	1551.00
Ni $2p_{3/2}$	–	–	–	857.85	857.95	–	–
Ni $2p_{1/2}$	–	–	–	875.65	too small	–	–
Ni 2p multiplet splitting	–	–	–	17.80	–	–	–
Ni LVV	–	–	–				
α′ (Ni)	–	–	–	411.75	411.75	–	–
				1699.70	1699.80	–	–

used to calculate E_a and the intercept gave ln (A/φ), were φ is the constant heating rate.

X-ray photoelectron spectroscopy (XPS)

All samples were dehydrated before X-ray photoelectron spectra were recorded using a VG Scientific ESCALAB Mk. II instrument. Non-monochromatic MgK_α (1253.6 eV) radiation was used. The base pressure was better than 10^{-10} mbar in the analyser. All samples were cooled to liquid nitrogen temperature and gold coated (approximately 1 nm thickness). The Au 4f XPS peaks were recorded for each sample and data were used to obtain static charge-corrected binding energies by means of the calibrated energy of 84.0 eV for the Au $4f_{7/2}$ peak maximum value [22–24]. Charge corrections varied between 6.40 and 8.00 eV. Linear background subtraction and a least-squares fitting procedure were used to determine peak positions.

Results

X-ray photoelectron spectroscopy (XPS)

The charge-corrected binding energies for the various peaks for the different oxalate compounds are listed in Table 4. The results correlate reasonably well with related literature values [25]. Some of the changes are very small and within the limits of accuracy of the instrument for the wider peaks (0.1 eV).

The Cu containing compounds

The generalization by Siegbahn *et al.* [26] that the higher the binding energy, the greater is the effective positive charge on a metal ion, is used to compare results. If the oxidation numbers are equal, positive shifts of binding energy values in the atom or ion under analysis, increase with increases in electronegativity of neighbouring atoms [27]. From the Cu 2p peak data it seems that the decreasing order of positive charge on the Cu ion in the different compounds is

$$NiCu(ox)_2 > Cuox \approx CoCu(ox)_2 \approx FeCu(ox)_2$$

Multiplet splitting (the energy difference between the two 2p peaks) is the result of spin interactions between unpaired electrons resulting from the photoionisation process and other unpaired electrons present in the system [9]. This separation between the two peaks also varies depending upon the environment

of the atom or ion concerned. Any neighbour that tends to decrease the electron density at the metal ion (increase positive charge), will decrease the splitting. According to this the decreasing order of positive charge on the Cu ion is

$$NiCu(ox)_2 > Cuox > CoCu(ox)_2 > FeCu(ox)_2,$$

although the multiplet splittings of the two middle compounds only differ by 0.05 eV.

The modified Auger parameter (α') is defined as the sum of the binding energy of the major photoelectron peak (e.g. Cu $2p_{3/2}$) and the kinetic energy of the major Auger peak (e.g. Cu $L_3M_{45}M_{45}$) [24]. The greater the Auger parameter, the more polarisable the ion in the compound. The change in Auger parameter is greater than the shift in binding energy and the Auger parameter is not dependent upon the charging effect. The decreasing polarisability of Cu in the different compounds is

$$NiCu(ox)_2 > Cuox > CoCu(ox)_2 > FeCu(ox)_2.$$

(This can also be seen as the decreasing order of possible positive charge on the Cu ions in the compounds.)

The Co containing compounds

The higher value of 782.60 eV for the Co $2p_{3/2}$ peak in Coox, in comparison with the value of 781.25 eV for the $CoCu(ox)_2$ compound, indicates that the cobalt ion in the mixed oxalate has a smaller effective positive charge than the cobalt ion in Coox. The copper ion thus increases the electron density around the cobalt ion, resulting (possibly) in a more covalent bond between the cobalt ions and the oxalate ions. This result is confirmed by the multiplet splittings and Auger parameters as summarized in Table 4.

The Fe containing compounds

Adding copper ions to the Feox compound results in a decreased positive charge on the iron ion, as can be observed from both the decreasing values of the Fe $2p_{3/2}$ peak values and the Auger parameter. A more covalent type of bond thus occurs in the mixed oxalate than in Feox.

The Ni containing compounds

Adding copper to Niox results in a more positive charge on the Ni ion, as indicated by the Ni $2p_{3/2}$ peaks and the Auger parameter. A more ionic bond (or a less covalent bond) between the Ni ion and the oxalate ions thus results.

Kinetic studies of the mixed oxalates

Programmed temperature TG and DSC curves for the mixed oxalates in N_2 and O_2 are given in Ref. [2]. The stoichiometries and thermochemistry are summarised in Table 1.

Iron-copper oxalate, $FeCu(ox)_2 \cdot 3H_2O$

Dehydration

Isothermal TG curves (130–145°C) were fitted by the contracting area equation (R2) ($\alpha = 0.3$–0.8) with an activation energy of 47±12 kJ·mol^{-1}. Isothermal DSC curves (145–170°C), converted to α-time curves, were initially approximately linear ($\alpha < 0.7$), followed by a deceleratory region. The linear region, approximated to a zero-order process, gave an activation energy of 80 ± 13 kJ·mol^{-1}. The deceleratory region could be fitted by the contracting area (R2) equation ($0.7 < \alpha < 0.99$), but the Arrhenius plot showed unacceptable scatter.

Kinetic analysis of the programmed temperature TG curve resulted in an activation energy of 92±1 kJ·mol^{-1}, using the R2 model ($0.1 < \alpha < 0.8$), and similar analysis of the programmed temperature DSC curves, using the R2 model, gave an activation energy of 90±1 kJ·mol^{-1}.

Results are summarized in Table 8. Values of the activation energy obtained for the dehydration of Feox were from 75 to 106 kJ·mol^{-1} (Table 2).

Decomposition

Examples of an α – time and a rate – time curve, derived from isothermal TG (270–285°C) experiments, are shown in Fig. 1. The decomposition of $FeCu(ox)_2$ is more complex than those of either the Co or Ni salts described below. From the rate-time traces, at 270 and 275°C, at least three processes could be distinguished, but at higher temperatures the second and third processes tended to merge. Values were selected for n_1, n_2, n_3, k_1, k_2, k_3, w_1, w_2 and w_3 for each isothermal experiment (270–285°C) as described above. Results are listed in Table 5. With so many adjustable parameters, values of the Avrami-Erofeev exponents, n_1, n_2 and n_3 were set initially = 3, and only adjusted if no other changes proved satisfactory. The weighting factors were adjusted independently, and $w_1+w_2+w_3$ is not necessarily =1. A residual slow decay was not included in the analysis. The weighting factor for the first process, w_1, was ap-

proximately constant at 5–8%. Rate – time curves at 280 and 285°C were initially described by two distinguishable concurrent processes plus a residual slow decay. The rate coefficients estimated for apparent process 2 (labelled 2*) in this way, however, showed little variation with temperature, and hence gave an apparent activation energy of effectively zero (Table 5). The large change in weighting factor, w_2, at the higher temperatures indicates the merging of processes 2 and 3 to give process 2*. In an attempt to improve the analysis, the first two values of k_2 and k_3 (i.e. at 270 and 275°C) were used to estimate the Arrhenius parameters of processes 2 and 3, and hence to estimated values expected for k_2 and k_3 at the higher temperatures (280 and 285°C). Rate-time curves at 280 and 285°C were then re-analyzed in terms of three processes. The calculated rate-time curve at 270°C is compared with experiment in Fig. 1. The estimated values of the Arrhenius parameters for the three processes are listed in Table 5.

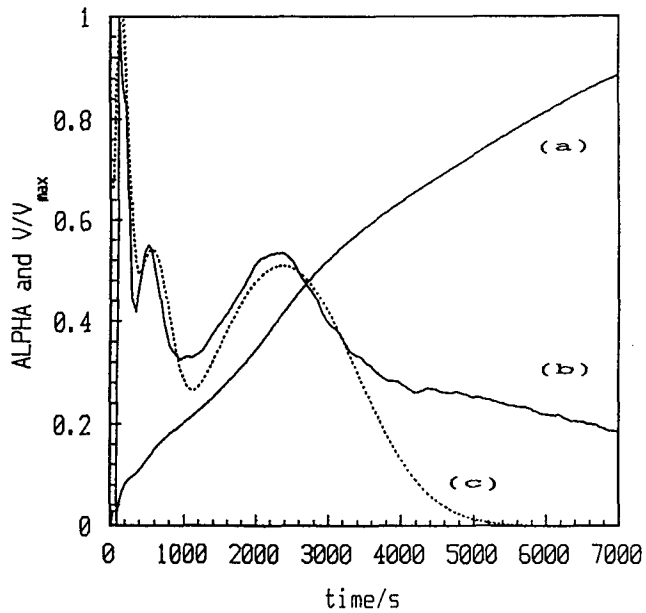

Fig. 1 Isothermal (270°C) experiments on the decomposition of $FeCu(ox)_2$. (a) α – time (from TG); (b) Experimental rate – time curve; (c) Calculated rate – time curve

From the α – time curves, it was only possible to distinguish between two processes. The final deceleratory stage (an overlap of process 2 and 3 above) of the α – time curve corresponded well with the contracting volume equation (R3) ($\alpha = 0.5$–0.8). The α values for this stage, for $\alpha < 0.5$, were masked by the

first reaction and could not be calculated. An Arrhenius plot for the second, faster reaction, gave an activation energy of 155±40 kJ·mol^{-1} (Table 9).

α – time curves, derived from isothermal DSC (290–320°C) experiments, were more regularly deceleratory (Fig. 1). It was not possible to isolate the individual decomposition steps and an overall activation energy of 61±10 kJ·mol^{-1} was obtained, using the R3 model, over a range of α = 0–0.9.

Kinetic analysis of the decomposition steps in the programmed temperature TG curve resulted in activation energies of 292±2 kJ·mol^{-1} and 202± 4 kJ·mol^{-1} for the first and second stage respectively. It was not possible to separate the two decomposition steps in the programmed temperature DSC curve and an overall activation energy of 253±3 kJ·mol^{-1} was obtained, over the range α = 0.2–0.9, assuming that the R3 model held.

Kinetic data obtained for the decomposition of $FeCu(ox)_2$ are summarised in Table 9.

Activation energies obtained from the programmed temperature TG or DSC experiments were similar to each other, but were considerably higher than values derived from isothermal experiments.

Cobalt-copper oxalate $CoCu(ox)_2 \cdot 3H_2O$

Dehydration

The α – time curves derived from isothermal TG (115–135°C) experiments were mainly deceleratory and the contracting-area equation (R2) gave the best fit (α = 0.2 –0.9) at all temperatures. The activation energy for dehydration was calculated as 130±9 kJ·mol^{-1}.

Isothermal (125 –150 °C) DSC curves, converted to α – time curves, were initially linear ($\alpha < 0.8$), after which they became deceleratory. The activation energy for dehydration, based on zero-order rate coefficients, was 89±5 kJ·mol^{-1}. The deceleratory stage of dehydration ($\alpha > 0.8$) could be fitted by the contracting area equation (R2), but the Arrhenius plot again showed unacceptable scatter.

An activation energy of 109±0.5 kJ·mol^{-1} was obtained from a Borchardt and Daniels [21] analysis of the programmed temperature DSC peak for the dehydration, assuming the applicability of the R2 model ($0 < \alpha < 0.8$). A similar analysis of the programmed temperature TG step for dehydration gave an activation energy of 118±2 kJ·mol^{-1} (R2 model).

Table 5 Rate parameters for the decomposition of $FeCu(ox)_2$ from isothermal TG

$T/^{\circ}C$	n_1	n_2	n_3	w_1	w_2	w_3	$k_1/10^{-3}s^{-1}$	$k_2/10^{-3}s^{-1}$	$k_3/10^{-3}s^{-1}$
270	3	3	3	0.08	0.11	0.45	3.3	1.32	0.35
275	3	3	3	0.07	0.09	0.44	3.5	1.46	0.43
280*	4	2.5		0.06	0.38	0.00	4.0	1.30	
285*	4	3		0.05	0.53	0.00	4.0	1.40	
280#	4	2.5		0.06	0.38	0.00	4.0	1.61#	0.53#
285#	4	3		0.05	0.53	0.00	4.0	1.77#	0.64#
280	4	2.5	3	0.06	0.32	0.30	4.0	1.40	0.50
285	4	3	3	0.05	0.45	0.20	4.0	1.50	0.64

Process	$E_a/kJ \cdot mol^{-1}$	$\ln(A/s^{-1})$	
1	35.9±8.7	2.23±0.04	
2*	3.0±14	-5.91±0.06	
2	49	4.27	(based on two
3	102	14.6	points only)

(Note: $t_o = 0$ at all temperatures; $w_1 + w_2 + w_3 \neq 1$)
(* refers to merged processes 2 and 3;
refers to values predicted from low temperature results)

Table 6 Rate parameters for the decomposition of $CoCu(ox)_2$

$T/^{\circ}C$	t_o/s	n_1	n_2	$k_1/10^{-3}s^{-1}$	$k_2/10^{-3}s^{-1}$	w_1	w_2
Isothermal TG							
300	0	4	2	1.7	0.369	0.23	0.77
310	0	4	2	2.4	0.317	0.34	0.66
320	60	5	1.8	3.2	0.484	0.34	0.66
330	300	5	2	6.5	0.650	0.29	0.71
340	24	5	2	9.0	1.285	0.37	0.63
Isothermal DSC							
325	0	2.2	2.0	2.5	0.9	0.115	0.58
330	0	2.5	2.2	3.1	1.37	0.145	0.58
**		5	2.0	4.65	0.714	0.30	0.70

Process	$E_a/kJ \cdot mol^{-1}$	$\ln(A/s^{-1})$
1	123±12	19.37±0.13
2	92±22	11.26±0.24

** values calculated at 330°C from TG results

Table 7 Rate parameters for the decomposition of $NiCu(ox)_2$

$T/^{\circ}C$	n_1	n_2	n_3	$k_1/10^{-3}s^{-1}$	$k_2/10^{-3}s^{-1}$	$k_3/10^{-3}s^{-1}$	w_1	w_2	w_3
Isothermal TG									
320	4	2		3.8	0.308		0.31	0.69	
325	4	2		3.7	0.381		0.33	0.67	
335	4	2		3.8	0.400		0.33	0.67	
345	5	2		3.8	0.791		0.30	0.70	
Isothermal DSC									
320	2	2	2	6.0	2.0	0.50	0.08	0.13	0.59
**	4	2	3	3.8	0.31	0.50	0.31	0.69	0.00

Process	$E_a/kJ \cdot mol^{-1}$	$\ln(A/s^{-1})$
1	1.4±2.4	-5.31±0.02
2	104±30	12.92±0.19

**values expected from TG at 320°C

Table 8 Dehydration of the mixed oxalates in nitrogen

Mixed oxalates	T_{range}/°C	Models		α-range	E_a/kJ·mol^{-1}	ln(A/s^{-1})
$FeCu(ox)_2 \cdot 3H_2O$						
isothermal TG	130–145	R2		0.3–0.8	47±12	6.8
isothermal DSC	145–170	Zero order	First stage	0.0–0.7	80±13	19.1
		R2	Second stage		24±31	–2.0
TG		R2		0.1–0.8	92±1	33.3
DSC		R2		0.1–0.8	90±1	34.0
$CoCu(ox)_2 \cdot 3H_2O$						
isothermal TG	115–135	R2		0.2–0.9	130±9	32.9
isothermal DSC	125–150	Zero order	First stage	0.0–0.8	89±5	19.8
		R2	Second stage		–24±10	
TG		R2		0.1–0.7	118±2	41.4
DSC		R2		0.0–0.8	109±1	39.1
$NiCu(ox)_2 \cdot 3.5H_2O$						
isothermal TG	165–185	R2		0.25–0.85	95±17	19.0
isothermal DSC	165–185	R2		0.01–0.9	86±16	0.9
TG		R2		0.1–0.85	98±1	32.7
DSC		R2		0.1–0.8	101±1	34.4

Results are summarized in Table 8. The value of the activation energy obtained for the dehydration of Coox was 158±1 kJ·mol^{-1} (Table 2).

Decomposition

Examples of an α – time and a rate – time curve, derived from isothermal TG (300–340°C) experiments, are shown in Fig. 2. On the basis of the rate – time curves, the reaction was analyzed in terms of two concurrent processes. The values selected for n_1, n_2, k_1, k_2, w_1, and w_2 and t_o for each isothermal experiment (300–340°C) on the decomposition of $CoCu(ox)_2$ are listed in Table 6. Except at the lowest temperature studied, the values of the Avrami-Erofeev exponents, n_1 and n_2, were approximately constant at 5.0 and 2.0, respectively. The weighting factor varied in a narrow range from 0.28 to 0.40. The values of k_1 and k_2 were used in conventional Arrhenius plots to give the Arrhenius pa-

rameters for the two processes listed in Table 6. The calculated rate-time curve at 330°C is included in Fig. 2.

The α – time curves also showed the overlap of two processes, an initial fast process and a slower process. The second, slow process could be described by the contracting volume equation (R3) over the range $\alpha = 0.6$–0.8. The α values for the second stage, for $\alpha < 0.5$, masked by the first reaction, were calculated from the R3 line. Values for the rate coefficient of the slow reaction were obtained from the slopes of the R3 lines, at various temperatures. These values were used in an Arrhenius plot, which resulted in an activation energy of 133±7 kJ·mol^{-1} for the slow reaction. This result was compared with the activation energy of 128±3 kJ·mol^{-1}, obtained using the initial slopes of the slow reaction, on the assumption that a rate equation of the form $(d\alpha/dt) = k(1-\alpha)^n$ applies, so that when α is small $(d\alpha/dt) \approx k$ or $\alpha \approx kt$. The activation energy of the fast reaction was obtained using the difference between the initial slopes of the total and slow reaction steps. An Arrhenius plot using these rate coefficients gave an activation energy of 178±39 kJ·mol^{-1}.

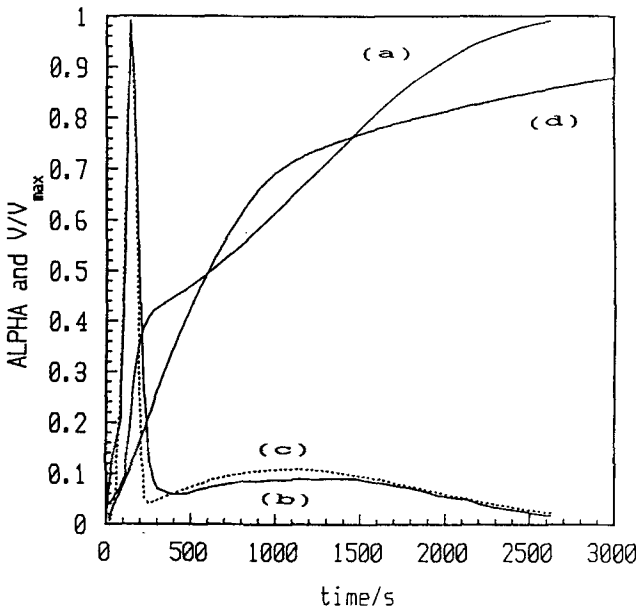

Fig. 2 Isothermal (330°C) experiments on the decomposition of $CoCu(ox)_2$. (a) α – time (from TG); (b) Experimental rate – time curve; (c) Calculated rate – time curve; (d) α – time (from DSC)

Table 9 Decomposition of the mixed oxalates in nitrogen

Mixed oxalates	T_{range}/ °C	Models		α range or stage	E_a/kJ·mol^{-1}	ln(A/s^{-1})
$FeCu(ox)_2$						
isothermal TG	270–300	R3		0.5–0.8	155±40	24.5
isothermal DSC	290–320	R3		0.0–0.9	61±10	3.9
TG		R3	First		292±2	67.5
			Second		202±4	45.9
DSC		R3		0.2–0.9	253±3	58.2
$CoCu(ox)_2$						
isothermal TG	300–340	R3		0.6–0.8	133±7	19.4
		initial rate				
		slow		<0.5	128±3	18.2
		fast		<0.5	178±39	29.2
isothermal DSC	325–345	Zero order	First	<0.5	92±39	11.0
		R3	Second	>0.5	101±16	10.8
TG		R3	First		221±2	52.1
			Second		325±5	69.4
DSC		R3		0.3–0.9	276±5	68.3
$NiCu(ox)_2$						
isothermal TG	330–345	R3		0.6–0.8	94±8	10.1
		initial rate				
		slow		<0.5	91±2	10.5
		fast		<0.5	145±24	22.1
isothermal DSC	320–340	Zero order	First	<0.7	75±42	7.2
			Second	0.7–0.95	12±2	–6.7
TG		R3	First		41±1	14.8
			Second		285±5	59.9
DSC		R3	First		175±3	43.6
			Second		227±4	52.9

The rate – time curves derived from isothermal DSC experiments (325 and 330°C) for the decomposition of $CoCu(ox)_2$, were analysed in terms of two concurrent processes, as described above, to obtain values for n_1, n_2, k_1, k_2, w_1

and w_2. The values obtained are also shown in Table 6 for comparison with values predicted from TG results at 330°C.

The α – time curves (Fig. 2 for an example) derived from isothermal (320–345°C) DSC experiments were initially approximately linear ($\alpha < 0.5$), followed by a deceleratory curve. The first stage of decomposition was therefore treated as a zero-order process and an activation energy of 92±32 kJ·mol^{-1} was obtained. The final stage of decomposition fitted the contracting volume (R3) equation well and resulted in an activation energy of 101±16 kJ·mol^{-1}. The thermal conductivity detector (TCD) indicated that only CO_2 was evolved during decomposition. The curve generated from the TCD results had approximately the same shape as the α-time curve, generated from DSC results.

It was not possible to distinguish between the two different decomposition steps in the programmed temperature DSC curves and an activation energy of 276±5 kJ·mol^{-1} was obtained for the overall reaction, assuming the applicability of the R3 model. In the programmed temperature TG curves, the two decomposition stages were separated. The R3 model was assumed and activation energies of 221±2 kJ·mol^{-1} and 325±5 kJ·mol^{-1} were obtained for the first and second steps, respectively.

The kinetic data, obtained for the decomposition of $CoCu(ox)_2$ in N_2 are summarised in Table 9.

The activation energy obtained for the first stage of decomposition from the programmed temperature TG experiment and the activation energy obtained from the programmed temperature DSC experiment are comparable, but values are again higher than those obtained from isothermal experiments.

Nickel-copper oxalate $NiCu(ox)_2 \cdot 3.5H_2O$

Dehydration

The α – time curves from isothermal TG (165–185°C) experiments, were fitted by the contracting area equation (R2) (α= 0.25–0.85). The activation energy for dehydration was 95±17 kJ·mol^{-1}. Isothermal (165–185°C) α – time curves from DSC experiments fitted the R2 equation well ($0.01 < \alpha < 0.9$) with an activation energy of 86±16 kJ·mol^{-1}.

The programmed temperature TG step for dehydration was analysed using the Borchardt and Daniels [21] method and the R2 model and gave an activation energy of 98±1 kJ·mol^{-1}. Similar analysis of a programmed temperature

DSC peak for the dehydration of NiCuox gave an activation energy of 101 ± 1 kJ·mol^{-1}.

Results are summarized in Table 8. The value of the activation energy obtained for the dehydration of Niox was 68 ± 15 kJ·mol^{-1} (Table 2).

Decomposition

The α – time and rate – time curves (Fig. 3 for an example) derived from isothermal TG (320–345°C) experiments for the decomposition of $NiCu(ox)_2$ were analyzed in terms of two processes. Table 7 lists the values of n_1, n_2, k_1, k_2, w_1 and w_2, selected for each isothermal experiment (320–345°C). Except for the higher temperature run at 345°C, the values of n_1 and n_2 were constant at 4.0 and 2.0, respectively. The weighting factors were approximately constant, with w_1 only varying between 0.30 and 0.33, and $w_2 = 1 - w_1$. The value of k_1 remained approximately constant at 0.0038 s^{-1}. The values of k_2 were used in an Arrhenius plot to give the values of the activation energy and A, shown in Table 8. Since the values of k_1 were approximately constant with change in temperature, the apparent activation energy for the first process, was approximately zero. The calculated rate-time curve at 320°C is also shown in Fig. 3.

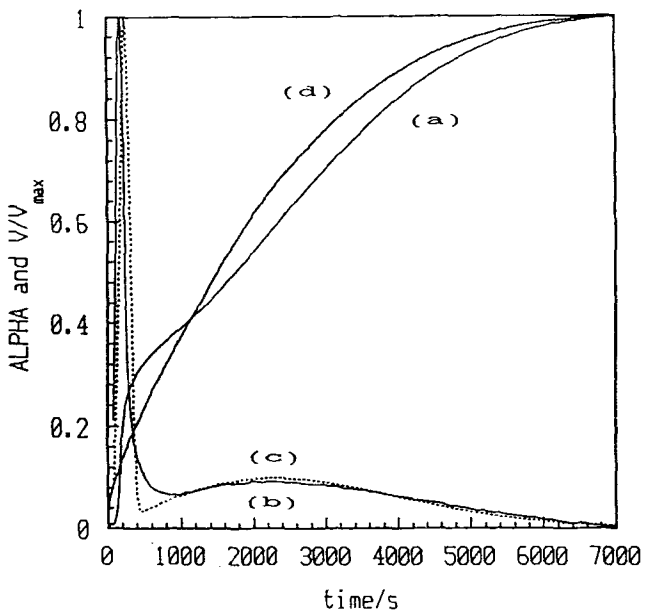

Fig. 3 Isothermal (320°C) experiments for the decomposition of $NiCu(ox)_2$. (a) α – time (from TG); (b) Experimental rate – time curve; (c) Calculated rate – time curve; (d) α – time (from DSC)

The α – time curves were analyzed by fitting the second, slow reaction to the R3 model ($\alpha = 0.5$–0.8). The values for the second stage, for $\alpha < 0.5$, were calculated from the R3 line. The slopes of the R3 lines, at various temperatures, were used in an Arrhenius plot, which gave an activation energy of 94±8 kJ·mol^{-1} for the slow reaction. An activation energy of 91±2 kJ·mol^{-1} was obtained using the initial slopes of the slow reaction ($\alpha < 0.5$), as discussed under $CoCu(ox)_2$. The rate coefficients for the fast reaction were obtained using the difference between the initial slopes of the total and slow reaction steps. An Arrhenius plot gave an activation energy of 145±24 kJ·mol^{-1}.

The isothermal (320°C) DSC curve consisted of three processes (Fig. 3) and the rate parameters, n_1, n_2, n_3, k_1, k_2, k_3, w_1, w_2 and w_3 estimated for these processes are listed in Table 7. They are compared with values estimated from an isothermal TG experiment at 320°C.

Isothermal (320–340°C) DSC runs on $NiCu(ox)_2$ were converted to α – time curves. The first stage of the curve ($\alpha < 0.7$) was linear. This was treated as a zero-order reaction and an activation energy of 75±42 kJ·mol^{-1} was obtained. The second stage of decomposition was fitted by the R3 equation and an activation energy of 12.0±1.5 kJ·mol^{-1} was obtained for the range $\alpha = 0.7$–0.9.

The gases evolved during the isothermal (345°C) decomposition of $NiCu(ox)_2$ were found to be both CO and CO_2. The α – time curves for the evolution of the two gases do not coincide, hence the composition of the gaseous mixture is changing with time and the heat effects measured by DSC will also be affected. The α – time curve, representing CO_2 evolution is deceleratory and corresponds approximately to the later part of the α – time curve generated from the DSC results, i.e. for $\alpha = 0.5$–1. The α – time curve for the evolution of CO reaches a plateau region at $\alpha = 0.8$ and the gradually increases again up to $\alpha = 1$. The approximate reaction stoichiometry is:

$$NiCu(ox)_2 \rightarrow 0.37Ni + 0.37Cu + 0.63(NiO + CuO) + 0.63CO + 3.37CO_2.$$

Kinetic analysis of programmed temperature TG curves resulted in an activation energy of 41±1 kJ·mol^{-1} for the first stage of decomposition and 285±5 kJ·mol^{-1} for the second stage. The R3 model was assumed. Similar analysis of the programmed temperature DSC curves (using the R3 model) gave activation energies of 175±3 kJ·mol^{-1} for the first step of decomposition and 227±4 kJ·mol^{-1} for the second step.

Results of the decomposition studies for $NiCu(ox)_2$ are summarized in Table 9. Again, there is agreement between the activation energy values obtained for the second stage of decomposition, from the programmed temperature TG and DSC experiments, but these values are considerably higher than values obtained from isothermal experiments.

Discussion

X-ray photoelectron spectroscopy

The decreasing order of electronegativity of the atoms concerned [28] is:

Ni (1.91 Paulings) > Cu (1.90) > Co (1.88) > Fe (1.83)

This is in agreement with the Cu XPS results where the decreasing order of positive charge on the Cu ion is:

$$CuNi(ox)_2 > Cuox > CuCo(ox)_2 > CuFe(ox)_2$$

Adding copper to Coox and Feox results in a more covalent type of compound, whilst adding copper to Niox results in a less covalent type of compound.

Isothermal DSC and isothermal TG

For a single rate process involving both mass and enthalpy changes, α-time curves calculated from isothermal TG (α = fractional mass change) and isothermal DSC (α = fractional enthalpy change) experiments should be identical. Differences can arrise form: (a) differences in the environment experienced by the sample in the two different instruments; or (b) different recorded sample temperatures arising from the different calibration procedures in TG and DSC.

When the rate process is complex, contributing processes will generally be accompanied by enthalpy changes of different magnitudes. Weighting factors for a complex DSC curve have to include enthalpy contributions for each process (and, for DTA, contributions allowing for different heat capacities of the contributing reaction systems).

Dehydrations

The dehydrations of the individual oxalates were generally found to be deceleratory processes, fitted by either the R2 or R3 models. The α – time curves for dehydration of the mixed oxalates were also mainly deceleratory and the

contracting area equation (R2) generally gave the best fit over the widest α range. Some α – time curves ($FeCu(ox)_2$ and $CoCu(ox)_2$), obtained from DSC experiments, showed a linear region for $\alpha < 0.7$, followed by a deceleratory region, up to $\alpha = 0.99$. The kinetic results for the dehydrations of the mixed oxalates are summarized in Table 8. The activation energies obtained using programmed temperature TG and DSC runs were in good agreement. Isothermal TG results are probably the least reliable owing to temperature calibration problems, especially at lower temperatures. There was reasonable agreement between E_a values obtained from the programmed temperature and isothermal DSC runs. Differences in the values of A obtained arise from the incorporation of various constants, including the heating rate, in this term, depending on the method of analysis.

Values of E_a for dehydration of the three mixed oxalates (Table 8) are very similar, i.e. not very dependent on the nature of M (Fe, Co, Ni), and are also similar to E_a values for the dehydration of the individual oxalates (Table 2). The temperature ranges giving comparable dehydration rates were broadly similar for all the hydrates (130 to 180°C).

Decompositions

Cuox

Copper oxalate is anhydrous and the programmed temperature TG curve in N_2 shows only one decomposition step of 55.9% in nitrogen, i.e. to Cu metal, with onset at ~290°C [2]. Decomposition is strongly exothermic ($\Delta H = -33$ kJ·mol^{-1}). A considerable amount of isothermal (240–280°C) kinetic information, obtained under a variety of conditions, has been reported (Table 3). Mohamed and Galwey [9] have recently provided evidence that the decomposition of Cuox proceeds via a Cu(I) intermediate with some overlap of stages. E_a is 140±7 kJ·mol^{-1} for the first stage and 180±7 kJ·mol^{-1} for the second.

Information on the decomposition of Feox was obtained in this study [5], and was compared with literature reports on the decomposition of the other individual oxalates. The isothermal decomposition of Feox in N_2 is mainly deceleratory (R3). The activation energy of 141±22 kJ·mol^{-1} is comparable with other values reported for the decomposition of Feox [10] and values for other oxalates, except the very high values for the decomposition of Niox and Cuox, reported by Mu and Perlmutter [6]. An apparent compensation effect was observed from the limited data.

Decompositions of the mixed oxalates, $MCu(ox)_2 \cdot xH_2O$, were all complex reactions, and that of M = Fe was the most complex. Isothermal rate time curves provided the most information about the early stages of reaction, which appear to involve overlapping sigmoid processes. These curves could be described by the Avrami-Erofeev model with different parameters for each contributing process. At the higher end of the range of isothermal temperatures used, the resolution of the contributing processes decreased and this could lead to anomalous results. For M = Fe these early processes generally had low activation energies (0–50 $kJ \cdot mol^{-1}$) and contributed from 20–50% of the overall rate. The deceleratory regions of the α – time curves could be fitted by the R3 model with higher activation energy: 61 $kJ \cdot mol^{-1}$ (DSC) to 155 $kJ \cdot mol^{-1}$ (TG).

Programmed temperature experiments, using either TG or DSC, generally gave considerably higher values for E_a than those obtained from isothermal experiments. This is an indication of the complexity of the reactions being examined. Isothermal studies at higher temperatures showed the decreased resolution of the concurrent processes, and such overlap will be even more marked under programmed temperature conditions. The agreement between the kinetic parameters from programmed temperature and isothermal experiments is better for the simpler processes involved in the reactions of the individual oxalates and for the dehydration of the mixed oxalates. For complex processes, agreement between kinetic parameters derived from TG and DSC results (and DSC and TCD results) cannot be expected to be good since thermal effects will not parallel mass changes, and for $NiCu(ox)_2$ the composition of the evolved gases was shown to change during the course of reaction.

$FeCu(ox)_2 \cdot 3H_2O$ was shown to contain coprecipitated Cuox [2]. Since the other mixed oxalates show two initial processes and $FeCu(ox)_2$ three, it is possible that the first process might be the decomposition of the Cuox impurity.

The decomposition of $NiCu(ox)_2$ was similar to that of $CoCu(ox)_2$, above, except that the first process, comprising of 30–33% of the total rate, had an apparent activation energy of approximately zero, while the activation energy for the second process was 104 $kJ \cdot mol^{-1}$.

The order of decreasing stability, as indicated by the temperature ranges giving comparable decomposition rates, was $NiCu(ox)_2 > CoCu(ox)_2 > FeCu(ox)_2$, which also corresponds to the order of increasing covalency as shown by XPS (see above).

Compensation effects

For many closely related reactions, a linear relationship (compensation effect [29]) is observed between the Arrhenius parameters for the individual reactions, i.e.

$$\ln A = BE_a + C$$

where B and C are constants.

The limited data available gave linear compensation plots for the dehydration of Feox, Coox and Niox, and for decomposition of Feox, Cuox and Coox. Niox was not included in the plot, since values of A, for decomposition in N_2 were not quoted in the literature. Reported values for activation energies of 665 $kJ \cdot mol^{-1}$ for the decomposition of Cuox and 766 $kJ \cdot mol^{-1}$ for the decomposition of Niox [6] are exceptionally high in comparison with values obtained by other authors and were therefore ignored.

Attempts have been made to give physical meaning to the parameters B and C in the compensation equation, above. Zsakó *et al.* [30] suggest that B characterizes the strength of the bond being broken when gaseous products are formed. The stronger the bond to be ruptured, the smaller the value of B. Parameter C is proposed [30, 31] to be related to the structure of, and defects in, the starting material, or to the mobility of constituents of the crystal lattice. According to this theory, the B value for the decomposition of the individual oxalates would be expected to be smaller than the B value for the dehydration of the individual oxalates. The compensation parameters for the dehydration and decomposition of the individual oxalates are summarized in Table 10. B has similar values for the decomposition and dehydration reactions. The compensation parameters for the dehydration and decomposition of the mixed oxalates are also listed in Table 10. B is smaller for the decomposition than for the dehydration of the mixed oxalates. Zsakó *et al.'s* [30] suggestion that the stronger

Table 10 Compensation parameters ($\ln A = BE_a + C$)

Reaction	B	C
1) The individual oxalates		
dehydration	0.291±0.010	–9.4±0.7
decomposition	0.285±0.004	–21.7±0.2
2) The mixed oxalates		
dehydration	0.260±0.16	9.9±2.1
decomposition	0.190±0.03	–4.8±2.1

the bond to be broken, the lower the value of B, is thus supported by the results for the mixed metal oxalates.

The variations observed in kinetic parameters reported for similar treatments of different preparations of the same compound, and from the use of different experimental techniques or kinetic analyses on a single preparation, usually do not allow any confident conclusions to be made.

References

1 D. Dollimore, Thermochim. Acta, 117 (1987) 331.
2 A. Coetzee, D. J. Eve and M. E. Brown, J. Thermal Anal., 39 (1993) 947.
3 D. Dollimore and D. L. Griffiths, J. Thermal Anal., 2 (1970) 229.
4 D. Broadbent, J. Dollimore, T. A. Evans and D. Dollimore, JCS Faraday Trans., 87 (1991) 161.
5 A. Coetzee, 'Thermal decomposition of mixed metal oxalates', MSc Thesis, Rhodes University, Grahamstown, South Africa 1993.
6 J. Mu and D. D. Perlmutter, Thermochim. Acta, 49 (1981) 207.
7 A. Venkataraman, N. V. Sastry and A. Ray, J. Phys. Chem. Solids, 53 (1992) 681.
8 D. Dollimore, T. A. Evans and Y. F. Lee, Thermochim. Acta, 194 (1992) 215.
9 M. A. Mohamed and A. K. Galwey, Thermochim. Acta, 217 (1993) 263.
10 M. A. Mohamed and A. K. Galwey, Thermochim. Acta, 213 (1993) 269.
11 D. Broadbent, D. Dollimore and J. Dollimore, J. Chem. Soc, A (1966) 1491.
12 A. Taskinen, P. Taskinen and M. H. Tikkanen, Reactivity of Solids, Proc. 8th Int. Symp., Plenum, New York 1977, p. 617.
13 P. W. M. Jacobs, A. R. Tariq Kureishy, Trans. Far. Soc., 58 (1962) 551; Reactivity of Solids, Proc 4th Int. Symp., Elsevier, Amsterdam 1961, p. 353.
14 D. A. Dominey, H. Morley, D. A. Young, Trans. Far. Soc., 61 (1965) 1246.
15 D. Broadbent, D. Dollimore, J. Dollimore, J. Chem. Soc, A (1966) 278.
16 J. Jach, M. Griffel, J. Phys. Chem., 68 (1964) 731.
17 E. G. Prout, M. E. Brown, Symposium on Chemical and Physical Effects of High Energy Radiation on Inorganic Substances, ASTM Spec. Tech. Pub. 359, (1964) 38.
18 A. Savitsky and M. J. E. Golay, Anal. Chem., 36 (1964) 1627.
19 M. E. Brown, D. Dollimore and A. K. Galwey, Comprehensive Chemical Kinetics, ed. C. H. Bamford and C. J. Tipper, Vol. 22, Elsevier, Amsterdam 1980, pp. 220–223.
20 M. E. Brown and A. K. Galwey, Anal. Chem., 61 (1989) 1136.
21 H. J. Borchardt and F. Daniels, J. Amer. Chem. Soc., 79 (1957) 41.
22 S. Strivastava, Polyhedron, 4 (1985) 11, 1925.
23 R. J. Bird and P. Swift. J. Electron Spectrosc., 21 (1980) 227.
24 I. J. Matienzo, L. I. Yin, S. O. Grim and W. E. Swartz, Inorg. Chem., 12 (1973) 12, 2762.
25 D. Briggs and M. P. Seah, Practical Surface Analysis by Auger and X-ray Photoelectron Spectroscopy, Wiley, New York 1983.
26 K. Siegbahn, C. Nordling, G. Johnson, J. Hedman, P. Hedan, K. Hamrin, U. Gelius, T. Bergmark, L. Werme, R. Manne and Y. Baer, ESCA, Applied to Free Molecules, North-Holland, Amsterdam 1969.
27 V. I. Nefedov, X-ray Photoelectron Spectroscopy of Solid Surfaces, VSP, Utrecht 1988.
28 R. C. Weast (Ed), Handbook of Chemistry and Physics, CRC Press, Florida,, 67th Edn, 1986.

29 A. K. Galwey, Advances in Catalysis, 26 (1977) 247.
30 J. Zsakó, Cs. Várhelyi and K. Szilágyi, J. Thermal Anal., 7 (1975) 41.
31 A. I. Lesnikovich and V. A. Levchik, J. Thermal Anal., 30 (1985) 677.

Zusammenfassung — Sowohl isotherme als auch programmierte Temperaturexperimente wurden zur Ermittlung der kinetischen Parameter der in Stickstoff erfolgenden Dehydratation und Zersetzung folgender Metallmischoxalate eingesetzt: $FeCu(ox)_2 \cdot 3H_2O$, $CoCu(ox)_2 \cdot 3H_2O$ und $NiCu(ox)_2 \cdot 3.5H_2O$ [*ox* = C_2O_4]. Die Ergebnisse wurden mit denen verglichen, die für die thermische Zersetzung der einzelnen Metalloxalate Cuox, $Coox \cdot 2H_2O$, $Niox \cdot 2H_2O$ und $Feox \cdot 2H_2O$ beschrieben wurden. Zur Untersuchung der Einzel- und Mischoxalate wurde auch Röntgenfotoelektronspektroskopie eingesetzt.

Die Dehydratationen der Mischoxalate sind hauptsächlich negativ beschleunigte Prozesse mit einer ähnlichen Aktivierungsenergie wie die individuellen hydratierten Oxalate (80–90 kJ/mol). Das Temperaturintervall für die Dehydratation ist für alle untersuchten Hydrate ähnlich (130 bis 180°C).

Die Zersetzungen der Mischoxalate waren alle komplexe endotherme Prozesse ohne sichtbare Ähnlichkeit mit der exothermen Reaktion von Cuox oder mit den Reaktionen der physikalischen Gemische der entsprechenden Einzeloxalate.

Die Stabilität, wie sie durch Temperaturintervalle zur Erzielung vergleichbarer Zersetzungsgeschwindigkeit gezeigt wird nimmt in der Reihenfolge $NiCu(ox)_2 > CoCu(ox)_2 > FeCu(ox)_2$ ab, was auch mit der steigenden Kovalenz der Cu–O-Bindung in dieser Reihenfolge übereinstimmt.